Journal of Applied Pharmaceutical Science Vol. 9(11), pp 069-077, November, 2019
Available online at http://www.japsonline.com
DOI: 10.7324/JAPS.2019.91109
ISSN 2231-3354

Molecular docking studies of bioactive compounds from the leaves of *Epiphyllum oxypetalum* against *Treponema pallidum*, Zika virus and liver cirrhosis

R. Abhishek Biswal, P. Jayashree, Kanna Mirunaalini, Vivek Pazhamalai*
Vels Institute of Science, Technology and Advanced Studies, Chennai, India.

ARTICLE INFO

Received 20/01/2019
Accepted 22/06/2019
Available Online: 04/11/2019

Key words:
PDB, *Treponema pallidum*, PDHK2, molecular docking.

ABSTRACT

The *Epiphyllum oxypetalum* is a unique plant that belongs to a cactaceae family. Traditionally, this plant mainly cures sexually transmitted diseases, liver infection, and antiviral disease. The molecular docking analysis was done against virulent bacterial and viral enzymes. The protein responsible for bacterial and viral disease were studied and retrieved from Protein Data Bank. The bioactive compounds of *E. oxypetalum* were docked against *Treponema pallidum*, liver cirrhosis, and Zika virus (ZIKV). The result obtained with better binding interactions against *T. pallidum* was Megastigmatrienone with −5.02Kcal/mol followed by liver cirrhosis was Megastigmatrienone with −4.58Kcal/mol and against ZIKV was Testerone cypionate with −7.84Kcal/mol. Thus, the molecular docking interactions shows better potential of inhibition against virulent enzymes and the bioactive compounds of *E. oxypetalum* leave which could be used as a lead for treating the diseases, such as Syphilis, liver cirrhosis, and ZIKV.

INTRODUCTION

Epiphyllum oxypetalum comes under the family of cactaceae. It is the one of the endogenous species with traditional valuable medicinal property. *Epiphyllum oxypetalum* is commonly known with several names, such as Brahma Kamal, Nishagandhi, and night blooming cereus. It is a unique plant used to treat liver infections, sexually transmitted disease, cancer, and urinary infection (Sousa *et al*., 2006). This plant kingdom mainly consists of large stretch of pharmacologically active molecules with derived medicinal properties. The stem of *E. oxypetalum* is used to cure dropsy and cardiac affections. A strong potent power of this plant is to neutralize the blood clotting factor. The whole plant plays a major role in curing microbial disease and viral disease with better inhibition factor. In modern era, Bioinformatics tools were applied to identify the potential targets for uncontrollable infections. Design of new compounds by modern strategies is done based on the known definition of therapeutic mechanism through modeling techniques increasing day by day with interest toward the new discovery of medicines. *In silico* approach helps in understanding the sites of molecular targets. The Gas Chromatography Mass Spectroscopy analysis of *E. oxypetalum* has been reported by (Dandekar *et al*., 2015) and was tabulated in Table 1. Different natural compounds, such as alkaloids, phenols, flavonoids, saponins, terpenoids, coumarins, quinones, and xanthones have been reported to have many biological activities. In this study, three commonly immune suppressing diseases were chosen that plays a vital role in killing the cell signaling molecules to deactivate the B cell and T cell lymphocytes.

Treponema pallidum

Syphilis is a chronic sexually transmitted disease caused by *T. pallidum* outbreak in Italy, Germany, United Kingdom, and France. This disease mainly gets benefited in the anus and vagina region or it will be most probably grown in mouth or in the rectum. This is motile Gram-negative spirochaete can be transmitted both sexually and from mother to child by suppressing the immune

*Corresponding Author
Vivek Pazhamalai, Vels Institute of Science, Technology and Advanced Studies, Chennai, India. E-mail: viveksncet2011 @ gmail.com

Table 1. Gas chromatography mass spectroscopy analysis of leaves of *E. oxypetalum*.

S. No	Compound	IUPAC name	Structure	Chemical formula
1.	4-Hydroxy-2-methylacetophenone	1-(4-hydroxy-2-methylphenyl)ethanone	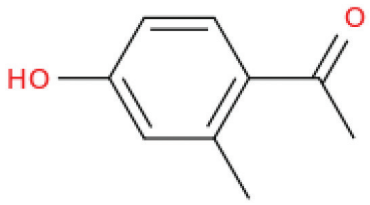	$C_9H_{10}O_2$
2.	Stigmasterol	(3S,8S,9S,10R,13R,14S,17R)-17-[(E,2R,5S)-5-ethyl-6-methylhept-3-en-2-yl]-10,13-dimethyl-2,3,4,7,8,9,11,12,14,15,16,17-dodecahydro-1H-cyclopenta[a]phenanthren-3-ol	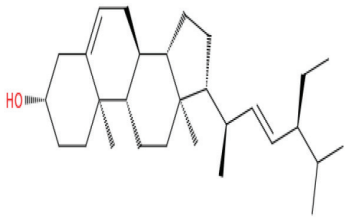	$C_{10}H_{12}O_3$
3.	6-Octen-1-ol, 3,7-dimethyl	3,7-dimethyloct-7-en-1-ol	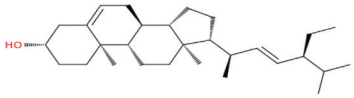	$C_{10}H_{20}O$
4.	Megastigmatrienone	(4Z)-4-[(E)-but-2-enylidene]-3,5,5-trimethylcyclohex-2-en-1-one	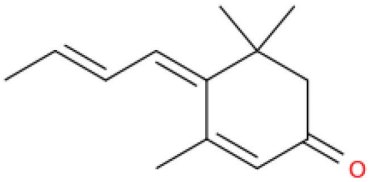	$C_{13}H_{18}O$
5.	Cyclohexylmethyl hexyl ester	cyclohexylmethyl hexyl sulphite	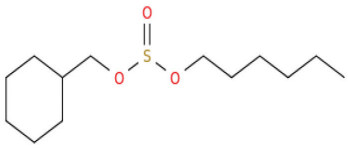	$C_{13}H_{26}O_3S$
6.	Testeronecypionate	[(8R,9S,10R,13S,14S,17S)-10,13-dimethyl-3-oxo-1,2,6,7,8,9,11,12,14,15,16,17-dodecahydrocyclopenta[a]phenanthren-17-yl] 3-cyclopentylpropanoate	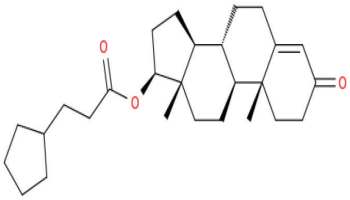	$C_{27}H_{40}O_3$

system. *Treponema pallidum* has long been regarded as a stealth pathogen because of its poorly antigenic and non-inflammatory surface (Fraser *et al*., 1998). There is now increasing evidence that the antigenic variation also contributes the ability of the spirochaete to evade host defences. The amino acids encoded with protein plays a vital role in enhancing the virulent factor of the disease by supplying sufficient nutrients and minerals that plays a major role in regulating cAMP (Deka *et al*., 2015; Schuppan *et al*., 1999).

Liver cirrhosis

Liver is a major organ of the human body. Viral hepatitis increases the chances for cirrhosis by affecting the liver inducing alkaline phosphatase enzymes which will be responsible for inhibiting the immune response. Individuals suffering from hepatitis are required to get regular check-ups because it is easily transmittable from one person to the other. It carries out a wide range of functions, such as digestion, adsorption and processing of food, detoxification of alcohol and drugs, and filtering of blood from the digestive tract (Amitrano *et al*., 2004). Liver cirrhosis is one of the major diseases prevalent in India. Liver cirrhosis is a degenerative liver disease involving four steps that results due to irreversible tissue scarring leading to cell death (Tsochatzis *et al*., 2014). Cirrhosis affects the abdominal blood vessels and the huge portal vein which transports blood from the intestines and spleen through the liver. Thus, blood finds alternative pathway to return to heart adding pressure on the blood vessels rupturing it and rendering its original function. Liver losses it's functioning capacity leading liver failure and eventually death in severe cases (Alberino *et al*., 2001; Dick *et al*., 1952).

Zika virus

Zika virus (ZIKV) is a flavivirus first isolated in 1948 from a senrinel rhesus monkey in the Zika forest of Uganda. Infection with this virus has been reported in Africa, India, Southeast Asia, and Micronesia. Recent phylogenetic analysis

of reported ZIKV strains has suggested that strains from Africa and Asia have emerged as two distinct virus lineages. ZIKV has been isolated from humans, nonhuman primates, and mosquitoes (Musso *et al*., 2015). This disease mainly relates with the blood cells of living organisms by resisting the antibody production and grows by benefiting itself. The clinical research confirmed that the ZIKV disease had titers of neutralizing antibodies against ZIKV that were at least four times as high as their titters of neutralizing antibodies against dengue virus (Faye *et al*., 2014; Lanciotti *et al*., 2008).

The current research work has been done to prove the inhibition potential of the novel drug compounds in the *E. oxypetalum* leaves by targeting the protein that is responsible for the *T. pallidum*, liver Cirrhosis and ZIKV disease.

MATERIAL AND METHODS

Selection and retrieval of protein structure from database

In this study, syphilis protein, namely, flavin traffling protein [Protein Data Bank (PDB) ID: 4XDR], from Cirrhosis protein, namely, pyruvate dehydrogenase kinase 2 (PDHK2) (PDB ID: 3CRK) and Zika E protein (PDB ID: 5UHY) were chosen. The correct crystal structure for these Syphilis, Cirrhosis, and ZIKV target has been obtained from Research Collaboratory for Structural Bioinformatics Data Bank.

Construction or retrieval of ligand structure

The bioactive compounds are chosen from the GC-MS analysis of *E. oxypetalum* leaves were used in this present study. Chem sketch is a chemically advanced quick drawing interface freeware, designed, and develop to design the structure of most ligands. Using the "draw mode" and then it was saved in the format of molecular file format. The other ligand structures were retrieved from Pub chem compound database (Lagunin *et al*., 2014).

Preparation of protein target

The virulent enzymes were studied and retrieved from the PDB. These proteins were commonly selected based on the suppression factor of human antibody against the diseases. These proteins (4XDR, 3CRK, and 5UHY) are mainly responsible for inducing immuno suppression diseases, such as syphilis, liver cirrhosis, and ZIKV. The hydrophobic molecules were removed along with the heteroatomic molecules. Single chain was determined for the docking analysis and was confirmed by visualizing in visualize software.

Molecular docking analysis

Docking is used to find the best matching between two molecules: a receptor and ligand. The various steps involved in Docking are as follows:

- Ligand preparation
- Receptor Preparation
- Binding Site preparation
- Scoring/Energy Evaluation

Molecular docking studies were performed for knowing the inhibition potential of drug molecules against Syphilis, ZIKV, and liver cirrhosis with bioactive compounds from the *E. oxypetalum* leaves using Auto Dock 4.2. It is an automated docking tool which works by Lamarckian Genetic Algorithm. The binding of molecules to a receptor with known 3D structure is predicted by Auto Dock 4.2 (Pal *et al*., 2006). The interaction of the molecules with their molecular targets forms the basis for drug development process. To perform docking experiment, the original protein were taken from the pdb file and the ligand pdb files from PRODRG server were submitted to AutoDock 4.2 for docking studies (Meenambiga *et al*., 2018). The binding energy is obtained for each ligand and the visual analysis of the docked complexes was done using Discovery studio Visulaizer 3.1 (Moroy *et al*., 2012; Muegge and Rarey, 2001; Walters, 2012).

Grid parameters

The default grid size in autodock software was set at 20 Å with grid points per map are 64,000. The default grid spacing was 0.375 Å with center grid box size at x axis −16.302, y axis −23.34, and z axis −16.245, respectively.

Lipinski's rule

All the compounds were selected on the basis of Lipinski's rule of five and compounds with any Ro5 violations were eliminated. It includes properties, such as molecular weight, lipophilicity, molar refractivity, number of hydrogen bond donors and acceptors

Discovery Studio Visualizer 3.1

Discovery Studio Visualizer is free software used for simulating and molecular modeling experiments for small and macromolecule. It generates 3D and 2D protein-ligand interaction plots. The ligand binding patterns are analyzed between the receptor protein and the ligand of interest (Singh and Romanowski, 1999).

Active sites representation of proteins

Treponema pallidum (4XDR)

Crystal structure of *T. pallidum* TP0796 Flavin trafficking protein, a bifunctional flavin mononucleotide (FMN) transferase/ flavin adenine dinucleotide (FAD) pyrophosphatase, D284A mutant, Area distribution node bound form. *Treponema pallidum* cause syphilis. Using modern molecular techniques, studying this species has become possible. TP0796 is a bacterial metal-dependent FAD pyrophosphatase of its kind (Giacani and Centurion-Lara, 2012). It hydrolyses FAD into AMP and FMN in the spirochete's periplasm. Orthologs of Ftp Tp from other bacteria appear to lack this hydrolytic activity; rather, they bind and flavinylate subunits of a cytoplasmic membrane redox system (Nqr/Rnf) (Radolf and Desrosiers, 2009). A single amino acid change in *T. pallidum* converts it from magnesium dependent FAD pyrophosphatase to an FAD-binding protein. Mutation in a metal binding residue reduces *T. pallidum* dual activity, thereby reducing the role of magnesium in enzyme-catalyzed reaction. 4XDR interacts selectively using non-covalent bonds with metal ion. It is present on the membrane that enables ease of interaction. The selective inhibitor and the active site presentation were shown in Figures 1 and 2.

Liver cirrhosis (3CRK)

Crystal structure of the PDHK2-L2 complex was taken from the data bank of protein. The activity of Pyruvate dehydrogenase

complex is regulated by PDHK. PDHK is a mitochondrial protein kinase carries out phosphorylation, which inactivates the entire compound. In humans, four closely-related protein kinases are present: PDHK1, PDHK2, PDHK3, and PDHK4, each have its unique function. PDHK2 is bound to the inner lipoyl-bearing domain of dihydrolipoamide transacetylase (L2) (Tsukamoto *et al*., 1995). PDHK2-L2 complex structure shows PDHK2 dimer bound to two L2 domains. R domain of PDHK-L2 complex composes of Ser12–Ala183, and the K domain encompasses residues His184–Tyr404. Residues of C-tail of the K domain contribute to the L2-bindind site of the PDHK2 molecule. The binding L2-site of PDHK2 is structured using amino acids of the R domain and one of PDHK2 dimer C-tail as well as amino acids of far carboxyl end present on the C-tail of the neighboring subunit of the dimer (Elbekai *et al*., 2004). PDHK2 and PDHK3 differ based on their lipoyllysine-binding cavities. These two structures display a novel type II potassium-binding site present on the PDHK2 interface consisting of L2 domain. Potassium ions binding at this interface plays a role in determining the strength of L2 binding. By comparing PDHK2-L2 complex structure with apo-PDHK2 it was found that the rearrangement within PDHK2 structure will affect the L2- and E1-binding sites (Marchette *et al*., 1969). The selective inhibitor and the active site presentation were shown in Figures 3 and 4.

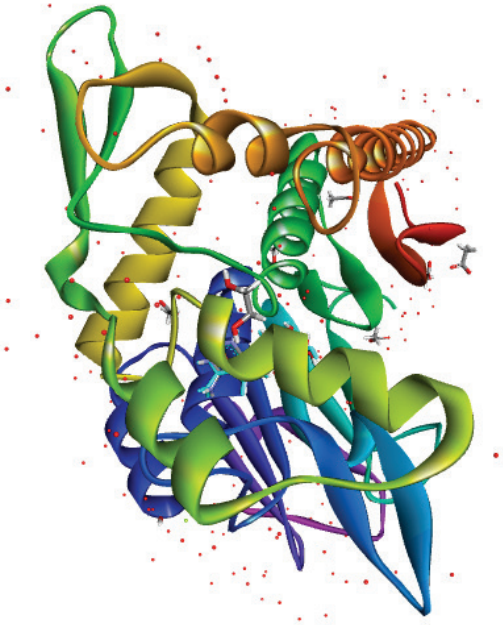

Figure 1. FAD protein, PDB ID:4XDR with chain A in complex with selective inhibitor.

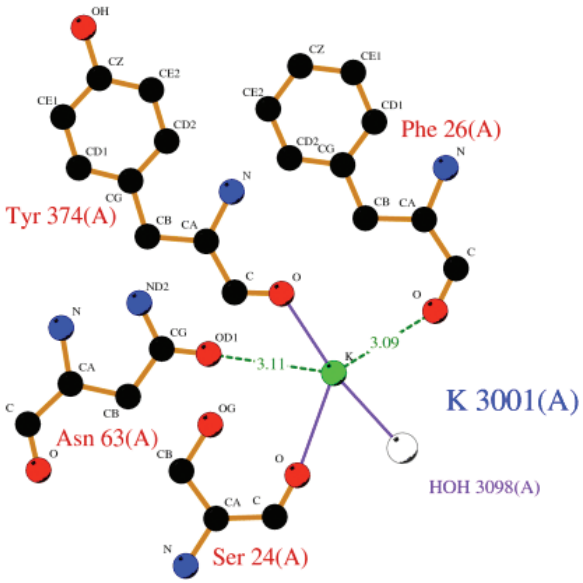

Figure 2. FAD in complex with selective inhibitors showing good active site region in asparagines (Asn) and tyrosine (Try).

Zika virus (5UHY)

Zika virus (ZIKV) is an epidemic disease linked with severe clinical manifestations, such as microcephaly in foetuses of infected pregnant women and Guillian–Barre syndrome in adults. Many antibodies have been synthesized to prevent and control ZIKV infection. This is an infectious ZIKV complex consisting of Fab fragment of a therapeutic and neutralizing monoclonal

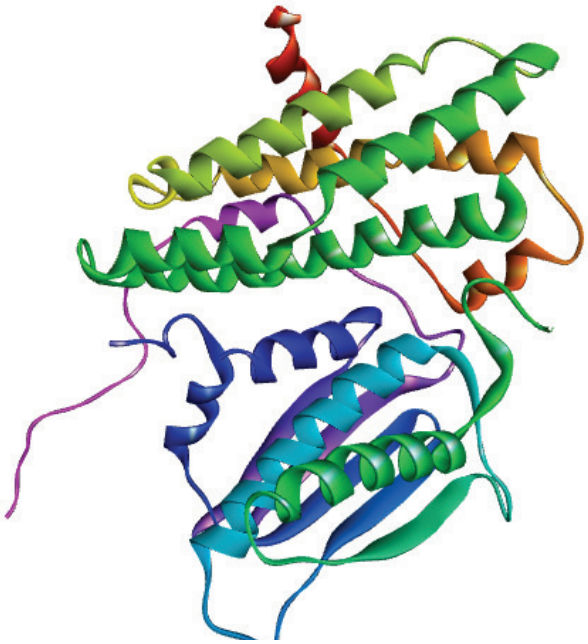

Figure 3. PDHK2 PDB ID: 3CRK with A and B chain in complex with selective inhibitor.

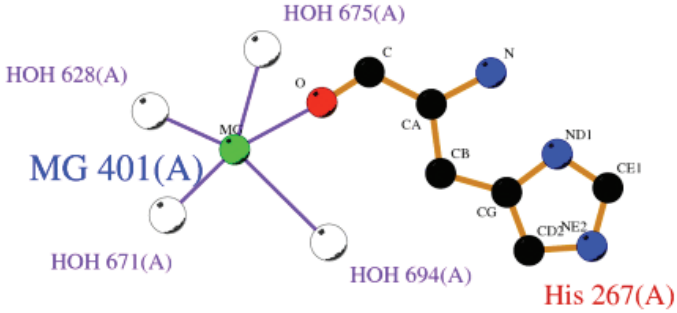

Figure 4. PDHK2 in complex with selective inhibitors showing good active site region Histone (His) and Trypsin (Trp).

antibody (Dai *et al*., 2017). This antibody has shown to reduce fetal infection and demise in mice in which the ZIKV-117 Fabs cross-links the monomers with the surface of E glycoprotein dimers as well as neighboring dimers (Ioos *et al*., 2014). The ZIKV-Fab surface extends from the surface of ZIKV. Fab site has two-fold, three-fold, and five-fold axes are labeled. It has asymmetric unit and icosahedral two-, three-, and five-fold axes. ZIKV surface has Fab binding sites A, C, and E. The A chains are arranges as dimer surrounding the icosahedral two-fold axis. C and E chains are arranged as general dimer around quasi two-fold axis. Asp67, Gln89, and Lys118 are present on the Fab binding site by mutagenesis (Calvet *et al*., 2016; Deka *et al*., 2015). The selective inhibitor was only being notified as shown in Figure 5.

RESULTS AND DISCUSSION

In silico studies of leaves of *E. oxypetalum* leaves were analyzed using Lipinski's rule of five followed by docking studies against three diseases Syphilis, ZIKV, and liver cirrhosis.

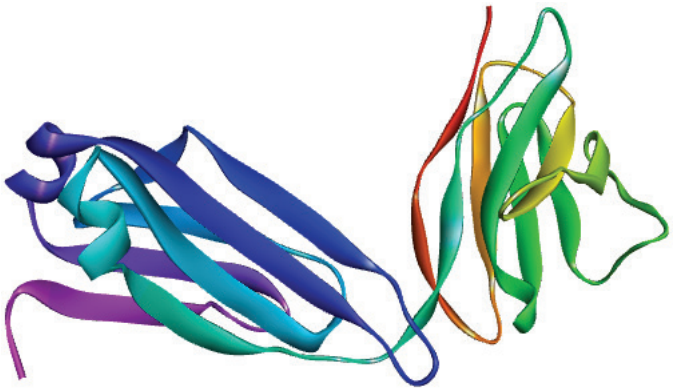

Figure 5. Envelope protein (E protein) PDB ID: 5UHY with A and B chain in complex with selective inhibitor.

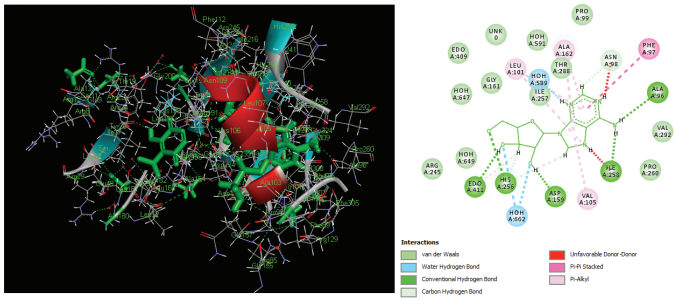

Figure 6. 3D and 2D residual interactions map of Megastigmatrienone against syphilis disease.

The compound satisfies the Lipinski rule of five as shown in Table 2. There are no research articles against *In vitro* studies of *E. oxypetalum* in these diseases. This research work reports the new novel drug that can be able to act as a potential inhibitor.

Treponema pallidum (4XDR)

For the 4XDR active site the binding energy for each ligand, hydrogen bond contacts, and other interactions were tabulated in Table 3. The megastigmatrienone shows the highest binding energy with the active site of 4XDR and docked conformation was shown in Figure 6 in which megastigmatrienone forms hydrogen bonds with ASN 98, ALA 258, ILE 258, ASP 159, and EDO 411 at the active site region of 4XDR protein that is represented as surface image in Figure 7. The binding efficiency with active site 3CRK protein was found to be good and strong and it has the aromatic and anti-bacterial activity against syphilis. The phenolic compound (4-hydroxy-2-methylacetophenome, 4-((1E)-3-Hydroxy-1-propenyl)-2-methoxyphenol), terpenoid compound 6-octen-1-ol,3,7-dimethyl) have found to be more potent with 4XDR through comparative analysis in this docking experiment.

Liver cirrhosis (3CRK)

The energy obtained by docked interactions with bond contacts and alternative interactions were shown in Table 4. The megastigmatrienone compound has the highest binding energy with the active site 3CRK protein and the docked conformations were shown in Figures 7 and 8. The C13 nor-isoprenoid derived from carotenoids (terpene) compound Megastigmatrienone

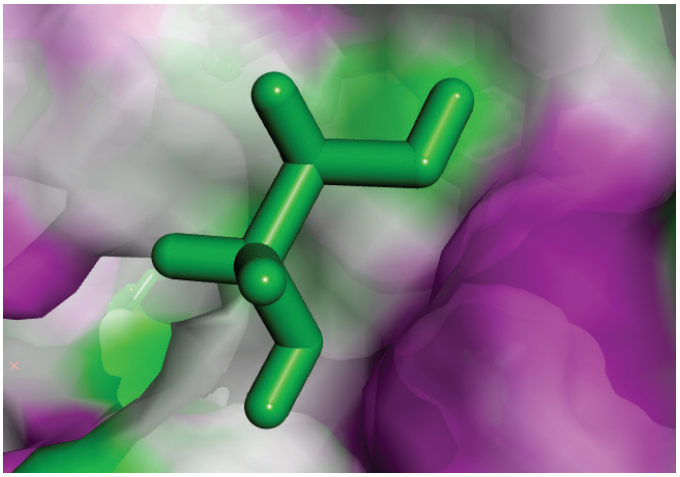

Figure 7. Surface structure of Megastigmatrienone.

Table 2. Lipinski's rule of five properties for the leaves of *E. oxypetalum*.

S. No	Phytochemical active compounds	Molecular weight (<500 Da)	Log *p* (<5)	Hydrogenbond (<5)	Hydrogen bond acceptor (<10)	Molecular refractivity (<130)
1.	4-Hydroxy-2-methylacetophenone	150	1.82	0	2	42.4
2.	Stigmasterol	180	1.55	1	3	48.2
3.	6-Octen-1-ol, 3,7-dimethyl	312	0.57	5	6	77.14
4.	Megastigmatrienone	190	3.83	0	1	59.5
5.	Cyclohexylmethyl hexyl ester	262	2.8	1	3	72.3
6.	Testerone cypionate	412	3.07	2	3	118.64

Table 3. Molecular docking analysis for leaves of *E. oxypetalum* against syphilis FAD protein (4XDR).

S. No	Compound name	Binding Energy	No. of vanderwaals interaction	No. of hydrogen bonds	Hydrogen bond interaction	Total polar and non-polar bondings
1.	4-Hydroxy-2-methylacetophenone	−3.98	PRO 99, ALA 162, THR 288, LEU 101, GLY 161, ARG 245, ASP 159, ILE 258, PRO 260, VAL 292, ALA 96, ASN 98	3	ALA 96, ILE 258, ASP 159	ALA 96, ILE 258, ASP 159, PRO 99, ALA 162, THR 288, LEU 101, GLY 161, ARG 245, ASP 159, ILE 258, PRO 260, VAL 292, ALA 96, ASN 98
2.	Stigmasterol	−4.54	THR 288, LEU 101, GLY 161, ARG 245, ASP 159, ILE 258, PRO 260, VAL 292, ALA 96, ASN 98	2	ALA 96, ILE 258	ALA 96, ILE 258, , THR 288, LEU 101, GLY 161, ARG 245, ASP 159, ILE 258, PRO 260, VAL 292, ALA 96, ASN 98
3.	6-Octen-1-ol, 3,7-dimethyl	−4.56	ILE 257, GLY 161, LEU 101, GLY 151, ASP 158, ALA 97, PRO 265	0		ILE 257, GLY 161, LEU 101, GLY 151, ASP 158, ALA 97, PRO 265
4.	Megastigmatrienone	−5.02	ALA 96, PHE 97, ASN 98, THR 288, ALA 162, THR 288, ILE 257, LEU 101, GLY 161, PRO 99, HOH 649, ARG 245, EDO 411, HIS 256, ASP 159, VAL 105, ILE 258, PRO 260	5	ASN 98, ALA 258, ILE 258, ASP 159, EDO 411	ALA 96, PHE 97, ASN 98, THR 288, ALA 162, THR 288, ILE 257, LEU 101, GLY 161, PRO 99, HOH 649, ARG 245, EDO 411, HIS 256, ASP 159, VAL 105, ILE 258, PRO 260
5.	Cyclohexylmethyl hexyl ester	−3.76	ALA 96, PHE 97, ASN 98, THR 288, ALA 162, THR 288, ILE 257, LEU 101, GLY 161, PRO 99, HOH 649, ARG 245, EDO 411, HIS 256, ASP 159, VAL 105, ILE 258, PRO 260	2	ALA 96, ASN 98	ALA 96, PHE 97, ASN 98, THR 288, ALA 162, THR 288, ILE 257, LEU 101, GLY 161, PRO 99, HOH 649, ARG 245, EDO 411, HIS 256, ASP 159, VAL 105, ILE 258, PRO 260
6.	Testerone cypionate	−1.02	ALA 96, VAL 292, PRO 260, ILE 258, VAL 258, VAL 105, ASP 159, HOH 662, HIS 256, EDO 411, HOH 649, ARG 245, GLY 161, LEU 101, EDO 409, HOH 591, ALA 162, ASN 98, PHE 97	5	ALA 96, ILE 258, ASP 159, HIS 256, EDO 411	ALA 96, VAL 292, PRO 260, ILE 258, VAL 258, VAL 105, ASP 159, HOH 662, HIS 256, EDO 411, HOH 649, ARG 245, GLY 161, LEU 101, EDO 409, HOH 591, ALA 162, ASN 98, PHE 97

Table 4. Molecular docking analysis for leaves of *E. oxypetalum* against liver cirrhosis (3CRK).

S. No	Compound name	Binding energy	No. of vanderwaals interaction	No. of hydrogen bonds	Hydrogen bond interaction	Total polar and non-polar bondings
1.	4-Hydroxy-2-methylacetophenone	−4.03	ILE 163, ARG 162, TYR 159, VAL 127, ILE 332, GLY 329, HIS 247	1	TYR 336	ILE 163, ARG 162, TYR 159, VAL 127, ILE 332, GLY 329, HIS 247, TYR 336
2.	Stigmasterol	−3.02	ARG 166, HIS 247, TYR 336, ILE 332, VAL 127, TYR 159, ILE 163	1	ARG 162	ARG 166, HIS 247, TYR 336, ILE 332, VAL 127, TYR 159, ILE 163, ARG 162
3.	6-Octen-1-ol, 3,7-dimethyl	−3.17	MET 167, ASN 170, HIS 244, TYR 336, HIS 247, ARG 162, ILE 163, SER 243	1	ARG 166	MET 167, ASN 170, HIS 244, TYR 336, HIS 247, ARG 162, ILE 163, SER 243, ARG 166
4.	Megastigmatrienone	−4.58	TYR 159, TYR 328, GLY 329, HIS 247, ILE 163, ILE 332, ARG 162, VAL 127	1	TYR 336	TYR 159, TYR 328, GLY 329, HIS 247, ILE 163, ILE 332, ARG 162, VAL 127, TYR 336
5.	Cyclohexylmethyl hexyl ester	−1.88	VAL 127, TYR 159, ARG 162, ARG 166, ILE 163, HIS 244, ILE 332, HIS 247, TYR 336, GLY 329	0	0	VAL 127, TYR 159, ARG 162, ARG 166, ILE 163, HIS 244, ILE 332, HIS 247, TYR 336, GLY 329
6.	Testerone cypionate	−4.05	ASN 170, SER 243, HIS 244, ILE 163, HIS 247, TYR 336, ARG 162, VAL 127, ILE 332, TYR 328, TYR 159, LEU 330, SER 333, GLU 251	1	GLY 329	ASN 170, SER 243, HIS 244, ILE 163, HIS 247, TYR 336, ARG 162, VAL 127, ILE 332, TYR 328, TYR 159, LEU 330, SER 333, GLU 251, GLY 329

Table 5. Molecular docking analysis for leaves of *E. oxypetalum* against ZIKV E protein (5UHY).

S. No	Compound name	Binding energy	No. of vanderwaals interaction	No. of hydrogen bonds	Hydrogen bond interaction	Total polar and non-polar bondings
1.	4-Hydroxy-2-methylacetophenone	−4.10	LYS 142, ASP 143, ILE 144, ASN 145, TRP 163	2	ILE 144, TRP 163	LYS 142, ASP 143, ILE 144, ASN 145, TRP 163
2.	Stigmasterol	−4.83	PRO 141, PHE 10, MET 11, LYS 103, GLU 105, SER 12, TYR 173, TYR 140, LYS 142, ASP 143	2	LYS 142, MET 11	PRO 141, PHE 10, MET 11, LYS 103, GLU 105, SER 12, TYR 173, TYR 140, LYS 142, ASP 143
3.	6-Octen-1-ol, 3,7-dimethyl	−4.49	TYR 173, PHE 10, LYS 142, TRP 163, ILE 144, THR 164, ASP 165	1	LYS 142	TYR 173, PHE 10, LYS 142, TRP 163, ILE 144, THR 164, ASP 165
4.	Megastigmatrienone	−4.66	LYS 103, GLU 105, GLN 166, ASP 165, THR 164, TYR 173, TRP 163, ASP 143, ILE 144, PHE 10, LYS 142	1	LYS 142	LYS 103, GLU 105, GLN 166, ASP 165, THR 164, TYR 173, TRP 163, ASP 143, ILE 144, PHE 10, LYS 142
5.	Cyclohexylmethyl hexyl ester	−4.11	PHE 10, PHE 139, ASP 143, ILE 144, LYS 142, TRP 163, THR 164, ASP 165, LYS 103, GLN 166, TYR 173, GLU 105	2	LYS 142, ILE 144	PHE 10, PHE 139, ASP 143, ILE 144, LYS 142, TRP 163, THR 164, ASP 165, LYS 103, GLN 166, TYR 173, GLU 105
6.	Testerone cypionate	−7.84	PHE 10, ASP 143, TYR 173, PHE 139, TRP 163, ILE 144, THR 164, ASP 165, GLN 166, GLU 105, LYS 142, LYS 142, LYS 103, LYS 9	2	LYS 142, GLU 105	PHE 10, ASP 143, TYR 173, PHE 139, TRP 163, ILE 144, THR 164, ASP 165, GLN 166, GLU 105, LYS 142, LYS 142, LYS 103, LYS 9

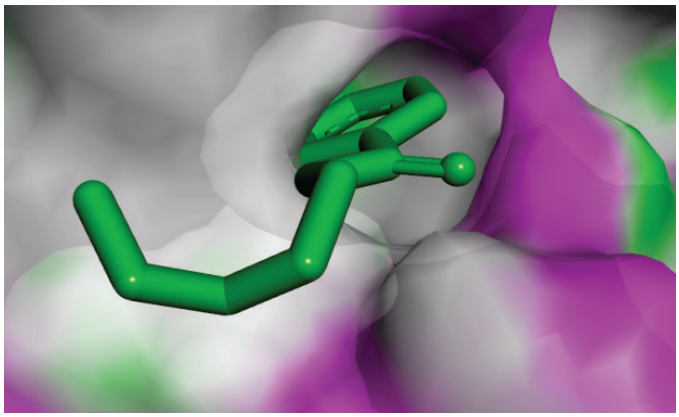

Figure 9. Surface structure of Megastigmatrienone.

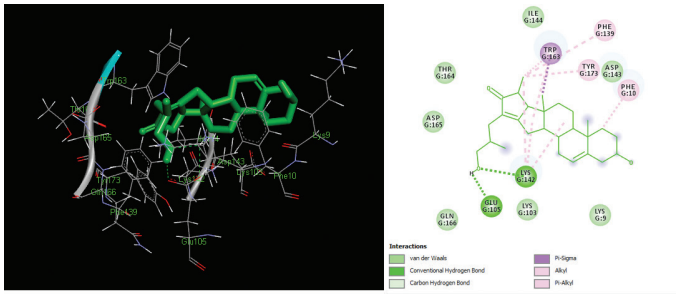

Figure 10. 3D and 2D residual interaction maps of Testeronecypionate against ZIKV.

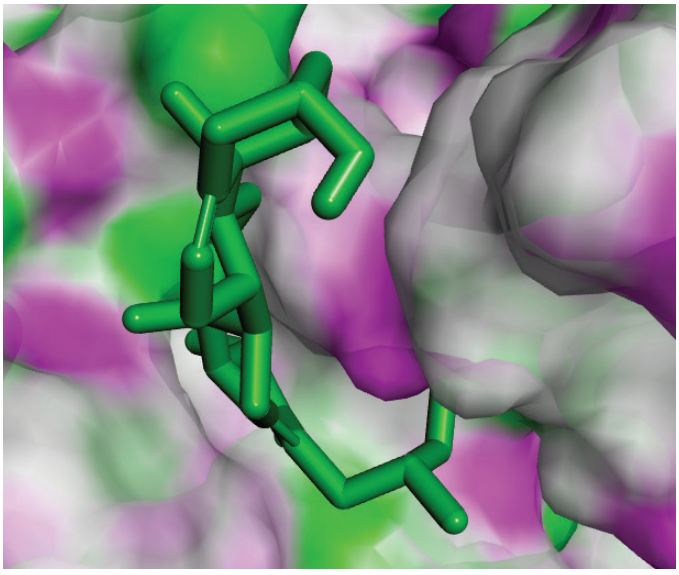

Figure 11. Docked confirmation of Testeronecypionate.

forms hydrogen bonds with TYR 336 at the active site region of 3CRK protein shown in Figures 8 and 9. The binding efficiency with active site 3CKR protein was found to be good and strong aromatic antiviral activity against liver cirrhosis. Thus, based on the molecular interaction analyzed and studied (Green *et al.*, 2014). The phenolic compound (4-hydroxy-2-methylacetophenome, 4-((1E)-3-Hydroxy-1-propenyl)-2-methoxyphenol), terpenoid compound 6-octen-1-ol,3,7-dimethyl) have found to be more potent with 3CKR through comparative analysis in this docking experiment.

Zika virus (5UHY)

For the 5UHY active site, the binding energy for each ligand, hydrogen bond contacts, and other interactions was described in Table 5. The steroid compound Testerone cypionate has the highest binding energy with the active site of 5UHY and docked conformation is in the Figures 10 and 11. The property

of the Testerone cypionate is replacing or supplementing the testosterone that is naturally made in the body. The binding efficiency of the 5UHY was found to be good with the bond interaction. Thus, this drug compounds shows better efficiency of the ZIKV with better molecular interactions (Cox *et al*., 2015). The phenolic compound 4-hydroxy-2-methylacetophenome, 4-((1E)-3-Hydroxy-1-propenyl)-2-methoxyphenol), terpenoid compound 6-octen-1-ol, 3, 7-dimethyl) have found to be more potent with 5UHY through comparative analysis in this docking experiment.

In this current study, docking results revealed the activity of compounds 3CKR, 5UHY, and 4XDR activity against the diseases liver cirrhosis, ZIKV, and Syphilis, respectively. In 3CKR protein active site, three hydrogen bonds are formed that works efficiently against liver cirrhosis due to its aromatic and anti-viral activity against the disease. 5UHY binding worked efficiently along with bond interaction that against ZIKV effectively (Muegge and Rarey, 2001; Saif *et al*., 2017). Megastigmatrienone had the highest binding energy with the active site of 4XDR. Among all the docked compounds the phenolic compound (4-hydroxy-2-methylacetophenome, 4-((1E)-3-Hydroxy-1-propenyl)-2-methoxyphenol), terpenoid compound 6-octen-1-ol,3,7-dimethyl)) have found to be more potent with 5UHY through comparative analysis in this docking experiment (Abdellatif *et al*., 2015). Furthermore it satisfies Lipinski's rule forming the base to use as an oral drug which can be initiated for further studies. In future, *in vitro* studies will be done for proof reading of the novel drug molecules against liver cirrhosis, ZIKV, and Syphilis.

ACKNOWLEDGMENT

The authors would like to thank Vels Institute of Science Technology and Advanced Studies (VISTAS) management for helping us to carry out this work.

CONFLICTS OF INTEREST

The authors declare that there are no conflicts of interest.

REFERENCES

Abdellatif AA, El Rasoul SA, Osman S. Gold nanoparticles decorated with octreotide for somatostatin receptors targeting. J Pharm Sci Res, 2015; 7:14–8.

Alberino F, Gatta A, Amodio P, Merkel C, Di Pascoli L, Boffo G, Caregaro L. Nutrition and survival in patients with liver cirrhosis. Nutrition, 2001; 17:445–50.

Amitrano L, Guardascione MA, Brancaccio V, Margaglione M, Manguso F, Iannaccone L, Grandone E, Balzano A. Risk factors and clinical presentation of portal vein thrombosis in patients with liver cirrhosis. J Hepatol, 2004; 40:736–41.

Calvet G, Aguiar RS, Melo AS, Sampaio SA, De Filippis I, Fabri A, Araujo ES, De Sequeira PC, De Mendonça MC, De Oliveira L, Tschoeke DA. Detection and sequencing of Zika virus from amniotic fluid of fetuses with microcephaly in Brazil: a case study. Lancet Infect Dis, 2016; 16:653–60.

Cox BD, Stanton RA, Schinazi RF. Predicting Zika virus structural biology: challenges and opportunities for intervention. Antivir Chem Chemother, 2015; 24:118–26.

Dai S, Zhao F, Zhang Q, Lau TK, Li T, Liu K, Ling Q, Wang C, Lu X, You W, Zhan X. Fused nonacyclic electron acceptors for efficient polymer solar cells. J Am Chem Soc, 2017; 139:1336–43.

Dandekar R, Fegade B, Bhaskar VH. GC-MS analysis of phytoconstituents in alcohol extract of *Epiphyllum oxypetalum* leaves. J Pharmacogn Phytochem, 2015; 4.

Deka RK, Brautigam CA, Liu WZ, Tomchick DR, Norgard MV. Evidence for posttranslational protein flavinylation in the syphilis spirochete *Treponema pallidum*: structural and biochemical insights from the catalytic core of a periplasmic flavin-trafficking protein. Mbio, 2015; 6:E00519–15.

Dick GW, Kitchen SF, Haddow AJ. Zika Virus (I). Isolations and serological specificity. Trans R Soc Trop Med Hyg, 1952; 46:509–20.

Elbekai RH, Korashy HM, El-Kadi AO. The effect of liver cirrhosis on the regulation and expression of drug metabolizing enzymes. Curr Drug Metab, 2004; 5:157–67.

Faye O, Freire CC, Iamarino A, Faye O, De Oliveira JV, Diallo M, Zanotto PM. Molecular evolution of Zika virus during its emergence in the 20th century. PLos Negl Trop Dis, 2014; 8:E2636.

Fraser CM, Norris SJ, Weinstock GM, White O, Sutton GG, Dodson R, Gwinn M, Hickey EK, Clayton R, Ketchum KA, Sodergren E. Complete genome sequence of Treponema pallidum, the syphilis spirochete. Science, 1998; 281:375–88.

Giacani L, Centurion-Lara A, Chattopadhyay S, Jeffrey BM, Le HT, Molini BJ, Lukehart SA, Sokurenko EV, Rockey DD. Footprint of positive selection in *Treponema pallidum* subsp. pallidum genome sequences suggests adaptive microevolution of the syphilis pathogen. PLoS Negl Trop Dis, 2012; 6:1698–701.

Green T, Grigorian A, Klyuyeva A, Tuganova A, Luo M, Popov KM. Structural and functional insights into the molecular mechanisms responsible for the regulation of pyruvate dehydrogenase kinase 2. J Biol Chem, 2008;283:15789–98.

Ioos S, Mallet HP, Goffart IL, Gauthier V, Cardoso T, Herida M. Current Zika virus epidemiology and recent epidemics. Med Mal Infect, 2014; 44:302–7.

Lagunin AA, Goel RK, Gawande DY, Pahwa P, Gloriozova TA, Dmitriev AV, Ivanov SM, Rudik AV, Konova VI, Pogodin PV, Druzhilovsky DS. Chemo-and bioinformatics resources for in silico drug discovery from medicinal plants beyond their traditional use: a critical review. Nat Prod Rep, 2014; 31:1585–611.

Lanciotti RS, Kosoy OL, Laven JJ, Velez JO, Lambert AJ, Johnson AJ, Stanfield SM, Duffy MR. Genetic and serologic properties of Zika virus associated with an epidemic, Yap State, Micronesia, 2007. Emerg Infect Dis, 2008; 14:1232–35.

Marchette NJ, Garcia R, Rudnick A. Isolation of Zika virus from *Aedes aegypti* mosquitoes in Malaysia. Am J Trop Med Hyg, 1969; 18:411–5.

Meenambiga SS, Venkataraghavan R, Biswal RA. In silico analysis of plant phytochemicals against secreted aspartic proteinase enzyme of *Candida albicans*. J Appl Pharm Sci, 2018; 8(11):140–50.

Moroy G, Martiny VY, Vayer P, Villoutreix BO, Miteva MA. Toward in silico structure-based ADMET prediction in drug discovery. Drug Discov Today, 2012; 17:44–55.

Muegge I, Rarey M. Small molecule docking and scoring. Rev Comput Chem, 2001; 17:1–60.

Musso D, Roche C, Robin E, Nhan T, Teissier A, Cao-Lormeau VM. Potential sexual transmission of Zika virus. Emerg Infect Dis, 2015; 21:359.

Pal SK, Bandyopadhyay S, Ray SS. Evolutionary computation in bioinformatics: a review. IEEE Transact Syst Man Cybern C Appl Rev, 2006; 36:601–15.

Saif LJ, Hou Y, Lin CM, Yokoyama M, Yount BL, Marthaler D, Douglas AL, Ghimire S, Qin Y, Baric RS, Wang Q. Deletion of a 197-amino-acid region in the N-terminal domain of spike protein attenuates porcine epidemic diarrhea virus in piglets. J Virol, 2017; 91:227–17.

Schuppan D, Afdhal NH. Liver cirrhosis. Lancet, 2008; 371(9615):838–51.

Singh AE, Romanowski B. Syphilis: review with emphasis on clinical, epidemiologic, and some biologic features. Clin Microbiol Rev, 1999; 12:187–209.

Sousa SF, Fernandes PA, Ramos MJ. Protein–ligand docking: current status and future challenges. Proteins, 2006; 65:15–26.

Tsochatzis EA, Bosch J, Burroughs AK. Liver cirrhosis. Lancet, 2014; 383:1749–61.

Tsukamoto H, Horne W, Kamimura S, Niemelä O, Parkkila S, Ylä-Herttuala S, Brittenham Gm. Experimental liver cirrhosis induced by alcohol and iron. J Clin Invest, 1995; 96:620–30.

Walters WP. Going further than Lipinski's rule in drug design. Expert Opin Drug Discov, 2012; 7:99–107.

How to cite this article:

Biswal RA, Jayashree P, Mirunaalini K, Pazhamalai V. Molecular docking studies of bioactive compounds from the leaves of *Epiphyllum oxypetalum* against *Treponema pallidum*, Zika virus and liver cirrhosis. J Appl Pharm Sci, 2019; 9(11):069–077.